frontiers | Frontiers in Earth Science

ORIGINAL RESEARCH
published: 24 May 2022
doi: 10.3389/feart.2022.870298

The Early Miocene Provenance Shift of ODP Site 1177 and Implications for the Tectonic Evolution of the Shikoku Basin, Philippine Sea Plate

*Wei Liu[1,2], Wanyi Feng[2], Congcong Gai[2], Yang Zhou[2], Yi Zhong[2], Wei Cao[2], Yuanjie Li[2], Xixi Zhao[2] and Qingsong Liu[2,3]**

[1]School of Environment, Harbin Institute of Technology, Harbin, China, [2]Center for Marine Magnetism (CM[2]), Department of Ocean Science and Engineering, Southern University of Science and Technology, Shenzhen, China, [3]Southern Marine Science and Engineering Guangdong Laboratory (Guangzhou), Guangzhou, China

The Ocean Drilling Program Site 1177 recovered the oldest (~23 Ma) sedimentary records in the Shikoku Basin, northeastern part of the Philippine Sea Plate. Changes in sediment provenances bear important implications for the tectonic evolution of the Philippine Sea Plate, but existing data are still controversial for the early Miocene. By integrating Sr-Nd isotopes, rock-magnetic parameters, diffuse reflectance spectroscopy, and the previous data on the detrital zircons and clay minerals from Site 1177, we found that a significant provenance shift occurred at ~16.5 Ma. The sediments of Site 1177 before ~16.5 Ma were mainly sourced from the Pearl River and Izu-Bonin Arc, but changed to the Yangtze River and Izu-Bonin Arc sources after that. This provenance shift was strongly linked with the northward motion and clockwise rotation of the Shikoku Basin in the Miocene, which marked the final time of separation between the Shikoku Basin and the South China Sea.

Keywords: ODP site 1177, provenance shift, philippine sea plate, tectonic, rock-magnetism

OPEN ACCESS

Edited by:
Monika Korte,
GFZ German Research Centre for Geosciences, Germany

Reviewed by:
Yongjian Yao,
Guangzhou Marine Geological Survey, China
David Buchs,
Cardiff University, United Kingdom

****Correspondence:***
Qingsong Liu
qsliu@sustech.edu.cn

Specialty section:
This article was submitted to Geomagnetism and Paleomagnetism, a section of the journal Frontiers in Earth Science

Received: *06 February 2022*
Accepted: *04 May 2022*
Published: *24 May 2022*

Citation:
Liu W, Feng W, Gai C, Zhou Y, Zhong Y, Cao W, Li Y, Zhao X and Liu Q (2022) The Early Miocene Provenance Shift of ODP Site 1177 and Implications for the Tectonic Evolution of the Shikoku Basin, Philippine Sea Plate. Front. Earth Sci. 10:870298. doi: 10.3389/feart.2022.870298

INTRODUCTION

The Philippine Sea Plate is uniquely located among the Eurasian, Pacific, and Indo-Australian plates, and is of great importance to fundamental plate tectonic theory and global tectonic evolution (Hall, 2002; Reagan et al., 2010; Wu et al., 2016; Maunder et al., 2020; Sibuet et al., 2021). The Philippine Sea Plate is not only a natural laboratory for the study of plate tectonics on aspects of initial subduction, arc rifting, and back-arc spreading (Reagan et al., 2010; Arculus et al., 2015; Maunder et al., 2020; Chen et al., 2021; Li et al., 2021) but is also significant for the tectonic reconstruction of the West Pacific and East Asia (Hall, 2002; Zahirovic et al., 2014; Lallemand, 2016; Wu et al., 2016; Ma et al., 2019; Queaño et al., 2020; Liu et al., 2021; Sibuet et al., 2021).

From west to east, the Philippine Sea Plate can be divided into the West Philippine Basin, Kyushu-Palau Ridge, Shikoku Basin, Parece Vela Basin, East Mariana Ridge, Mariana Trough (or Mariana Back-Arc Basin), and Izu-Bonin-Mariana Arc (**Figure 1**). The seafloor spreading of the West Philippine Basin was thought to have started from 51 Ma (Ishizuka et al., 2013), 55 Ma (Deschamps and Lallemand, 2002), or 58 Ma (Hilde and Lee, 1984) to 36–34 Ma (Sasaki et al., 2014) or 33–30 Ma (Deschamps and Lallemand, 2002). The Kyushu-Palau Ridge was a remnant arc, which was ever connected to Izu-Bonin-Mariana Arc before the back-arc spreading of the Shikoku Basin and Parece Vela Basin at 30–15 Ma (Okino et al., 1999; Sdrolias et al., 2004). The Mariana Trough was a back-arc basin, which has been spreading since ~7 Ma (Hussong and Uyeda, 1982; Yamazaki et al., 2003).

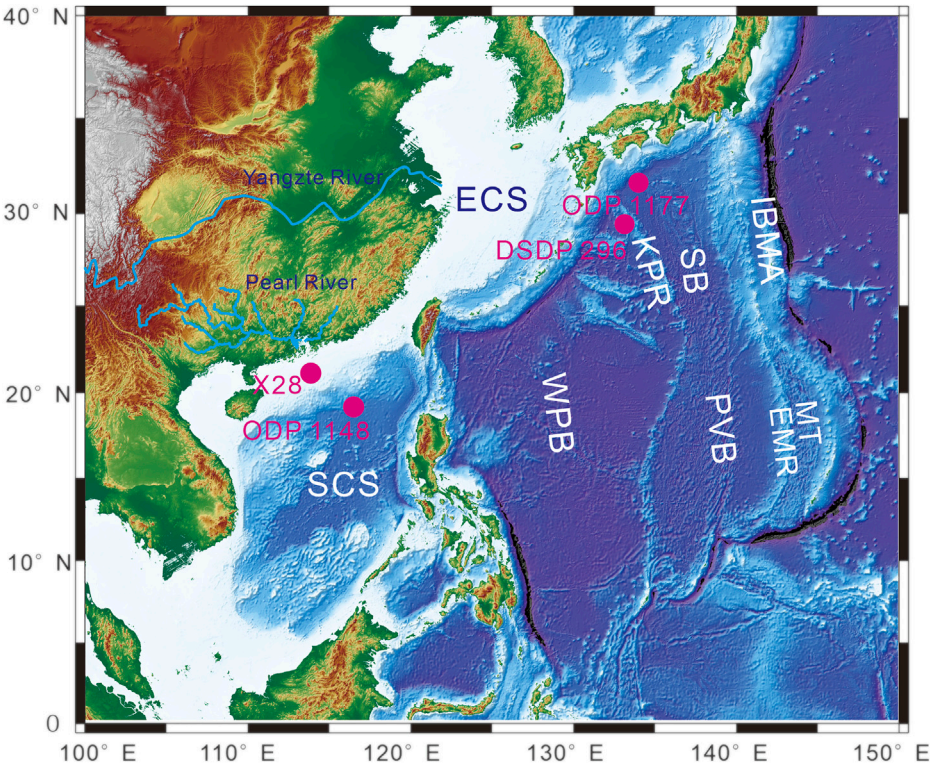

FIGURE 1 | Schematic map showing the studying area. Sites mentioned in this study are indicated by the purple circles. SCS = South China Sea, WPB = West Philippine Basin, KPR = Kyushu-Palau Ridge, SB = Shikoku Basin, PVB = Parece Vela Basin, EMR = East Mariana Ridge, MT = Mariana Trough, IBMA = Izu-Bonin-Mariana Arc, ECS = East China Sea.

The Ocean Drilling Program (ODP) Site 1177 recovered cores from the early Miocene to Pliocene sedimentary succession, which was the oldest sedimentary record in the Shikoku Basin. Thus, the study of Site 1177 provenance can shed light on the Miocene tectonic evolution of the Shikoku Basin, even the Philippine Sea Plate. Previous studies have constructed the tectonic evolutionary models of the Philippine Sea Plate based on evidences from paleomagnetism (Louden, 1977; Kinoshita, 1980; Keating, 1981; Keating and Herrero, 1981; Bleil, 1982; Haston and Fuller, 1991; Haston et al., 1992; Koyama et al., 1992; Hall et al., 1995; Queano et al., 2007; Yamazaki et al., 2010, 2021; Richter and Ali, 2015; Liu et al., 2021), submarine magnetic anomaly (Okino et al., 1999; Sdrolias et al., 2004), seismic tomography (Zahirovic et al., 2014; Wu et al., 2016; Ma et al., 2019; Sibuet et al., 2021) and sedimentary provenance (Clift et al., 2013; Saitoh et al., 2015), etc. Researchers agreed on the first-order evolution that the Philippine Sea Plate moved ~20°northward from the equator to the present position and simultaneously rotated ~90°clockwise since the Eocene (Hall, 2002; Yamazaki et al., 2010; Zahirovic et al., 2014; Wu et al., 2016; Ma et al., 2019; Liu et al., 2021). However, the details of the evolution of the Philippine Sea Plate are still needed to be clarified, especially for the Shikoku Basin.

The evolution of provenance can be used to constrain plate tectonics by examining different spatio-temporal relationships of the source to sink (Clift et al., 2013; Saitoh et al., 2015). Some work on early Miocene provenance analyses has been performed for sediments from Site 1177; however, there are still controversies. For example, based on the lithological similarity between Site 1177 and Site 296, Shipboard Scientific Party (2001) thought that the sedimentary materials of Site 1177 most likely originated from the Kyushu-Palau Ridge, and they also did not rule out the small possibility of sources from Japan. However, the results from Shipboard Scientific Party (2001) are preliminary, and the interpretations were tentative. In a post-cruise study, Underwood and Fergusson (2005) identified large amounts of smectite from Site 1177 mudstones in the early Miocene. Given that the Izu-Bonin Arc is mainly composed of basalt, which contributes greatly to the formation of smectite (Fagel et al., 2001), Underwood and Fergusson (2005) speculated that the early Miocene provenance might derive from the Izu-Bonin Arc. Recently, Liu et al. (2021) suggested that the silt turbidites from Site 1177 were sourced from the Pearl River on the basis of similar zircon age spectra between Site 1177 and Site X28 (**Figure 2C**).

These differences in provenance interpretation arose from at least two aspects. On the one hand, the research materials are different. Mudstones (Underwood and Fergusson, 2005) and turbidites (Liu et al., 2021) in the sedimentary sequence experienced different sedimentary processes and, therefore, may have originated from different sources. On the other hand, the above-mentioned studies are generally based on a certain method but lack comprehensive analysis. Therefore, it is necessary to integrate multiple methods to re-evaluate provenance evolution.

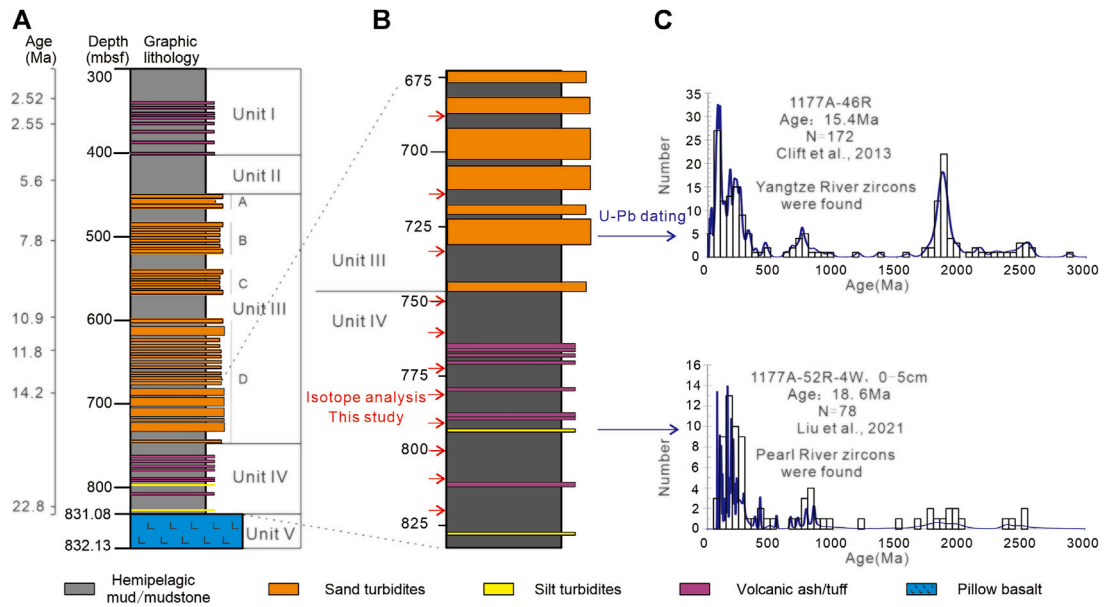

FIGURE 2 | (A) The stratigraphic column of ODP Site 1177. A, B, C, and D in Unit III represented four sand packets. mbsf = meters below seafloor. **(B)** A larger version of Panel 2A between 675 and 831 m. The red arrows indicate locations of 11 mudstone samples that Sr-Nd isotope experiments were conducted in this study. **(C)** The zircon age spectrum of turbidites from Site 1177. The blue arrows indicate locations of turbidites that zircon U-Pb dating experiments were performed in the previous study. The silt turbidites were sourced from the Pearl River at ~18.6 Ma (Liu et al., 2021), and the Yangtze River zircons were found in the sand turbidites at ~15.4 Ma (Clift et al., 2013).

The Nd isotope is resistant to the processes of weathering, denudation, transportation, and deposition, which could preserve reliable provenance information (Goldstein and Jacobsen, 1988; Wei et al., 2012). Generally, the plots of Sr-Nd isotopes are sensitive in tracking the different provenances (Clift et al., 2014). The magnetic minerals in the sediments can also be used to distinguish provenance according to the variations in the type, concentration, and grain size of magnetic minerals (Liu et al., 2012). Specifically, the *L*-ratio, proposed by Liu Q. et al. (2007), is very sensitive to provenance changes. The larger the *L*-ratio, the 'harder' (higher-coercivity) the magnetic minerals (Liu Q. et al., 2007). Diffuse reflectance spectroscopy (DRS) can be used to identify the properties and concentrations of goethite (Gt) and hematite (Hm) (Scheinost, 1998; Hu et al., 2016).

In this study, we integrated new Sr-Nd isotope, rock-magnetic parameter, and DRS data from mudstones from ~22 Ma to ~14 Ma, as well as published provenance data of detrital zircons and clay minerals, to conduct a comprehensive provenance analysis of Site 1177, which could reconcile the previous provenance disputes. Moreover, if the turbidites were derived from the Pearl River and Yangtze River at ~18.6 Ma and ~15.4 Ma, respectively, this would imply a provenance shift between 18.6 Ma and 15.4 Ma. When did the provenance shift occur? Was the provenance shift attributed to tectonic events in the Philippine Sea Plate? A comprehensive provenance study can answer the above questions and deepen the understanding of the provenance and tectonic evolution of the Shikoku Basin.

MATERIALS AND METHODS

Materials

To study the deformation and related fluid flow processes of the accretionary prism in the Nankai Trough, Sites 1173–1178 during ODP Leg 190 were drilled. Among these sites, Site 1177 (31° 39′N, 134° 0′E, 4,844 m water depth) yields the oldest sedimentary rocks in the northern Sikoku Basin. It consists of a sedimentary record between 300 m below seafloor (mbsf) and 831.08 mbsf, and a basalt basement with a thickness of 1 m (**Figure 2A**). The sediments from Site 1177 are muds, silts, sands, and volcanic ashes, which gradually consolidated downward into sedimentary rocks. Site 1177 is divided into five units based on lithologic assemblages (Shipboard Scientific Party, 2001). Unit I is interpretated as upper Shikoku Basin hemipelagic facies, while Units II and III are described as lower Shikoku Basin hemipelagic facies and turbidite facies, respectively. Unit IV represents volcaniclastic-rich facies and Unit V is the basalt basement. In Units III and IV, the zircon age spectrum of turbidites was determined (Clift et al., 2013; Liu et al., 2021) (**Figure 2C**). The results indicated that the Pearl River zircons were found in the silt turbidites at ~ 18.6 Ma and the Yangtze River zircons were found in the sand turbidites at ~15.4 Ma. In this investigation, we aimed to analyze the provenance evolution of mudstones in Units III and IV from 821 mbsf (~22 Ma) to 687 mbsf (~14 Ma) (**Figure 2B**). The age of each sample was determined by linear interpolation based on the magnetostratigraphic and biostratigraphic ages (Shipboard Scientific Party, 2001).

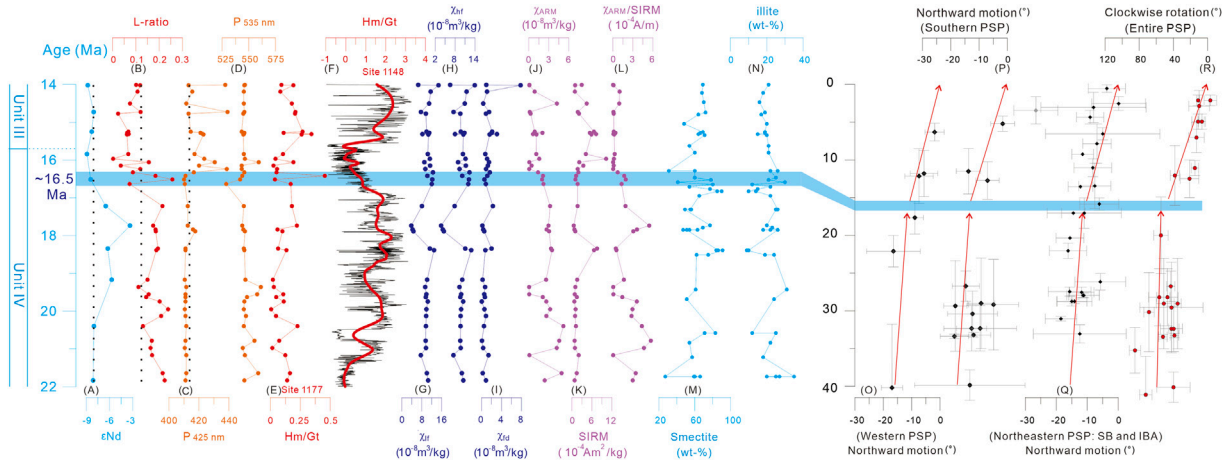

FIGURE 3 | The temporal variations of isotopic and rock-magnetic parameters between ~14 Ma and ~22 Ma: **(A)** εNd, **(B)** *L*-ratio, **(C)** $P_{425\ nm}$, **(D)** $P_{535\ nm}$, **(E)** Hm/Gt of Site 1177, **(F)** Hm/Gt of Site 1148 (Clift et al., 2014), **(G)** χ_{lf}, **(H)** χ_{hf}, **(I)** χ_{fd}, **(J)** χ_{ARM}, **(K)** SIRM, **(L)** χ_{ARM}/SIRM, **(M)** smectite, and **(N)** illite (Steurer and Underwood, 2003; Underwood and Fergusson, 2005). The northward motion of **(O)** the western PSP (Queano et al., 2007), **(P)** the southern PSP (Hall et al., 1995), **(Q)** the northeastern PSP (DSDP and ODP sites in the SB and IBA: sites 442, 782, 784, 786, 787, 792, 793, and 1177) (Kinoshita, 1980; Haston and Fuller, 1991; Haston et al., 1992; Liu et al., 2021), and **(R)** the clockwise rotation of the PSP (Haston and Fuller, 1991; Queano et al., 2007). The blue thick lines mark the sudden changes in geochemical, rock-magnetic, and spectral parameters, and tectonic movement of the PSP. The red lines in **(O–R)** are used to visualize the tectonic movement trends. PSP = Philippine Sea Plate, SB = Shikoku Basin, IBA = Izu-Bonin Arc.

Methods

Together, 11 mudstone samples were selected to conduct Sr-Nd isotope analysis. The detailed analytical procedures were the same as those described by Wei et al. (2012). In the pre-treatment, we firstly removed the biogenic carbonate with 2 N HAc, and then the samples were centrifuged, dried and crushed into powders. Next the powders were heated to remove the organic materials at 700°C, digested by an HNO_3+HF acid mixture, and dissolved in a 2 N HCl solution. Finally, a MicroMass Isoprobe multi-collector–inductively coupled plasma–mass spectrometer (MC–ICP–MS) were used to determine the Sr-Nd isotope data.

The mass-specific magnetic susceptibility (χ), anhysteretic remanent magnetization (ARM), isothermal remanent magnetization (IRM) and DRS of 38 mudstone samples were measured. The susceptibility was measured at dual frequencies of 976 Hz (χ_{lf}) and 15616 Hz (χ_{hf}). The frequency-dependent susceptibility is defined as $\chi_{fd} = \chi_{lf} - \chi_{hf}$. The ARM was induced in a peak alternating field of 100 mT with a 50 μT direct current field, which was normalized to ARM susceptibility (χ_{ARM}). The IRM was firstly acquired by an ASC IM10-30 Impulse Magnetizer in a 1000 mT direct current field, which was regarded as saturation IRM (SIRM). Then reverse fields of −100 mT and −300 mT were used for demagnetization, which corresponded to IRM_{-100mT} and IRM_{-300mT}, respectively. The $(SIRM + IRM_{-300mT})/(SIRM + IRM_{-100\ mT})$ was calculated to determine the *L*-ratio (Liu Q. et al., 2007).

DRS measurements were conducted by a Cary 5000 spectrophotometer with the same methods as used by Hu et al. (2016). The second derivatives of the Kubelka-Munk functions were used to determine the band positions of Hm and Gt, which are ~535 nm ($P_{535\ nm}$) and ~425 nm ($P_{425\ nm}$), respectively. Because of Al substitution, the position of $P_{535\ nm}$ and $P_{425\ nm}$ might vary (Hu et al., 2016). We choose the locations nearest to 535 and 425 nm to define $P_{535\ nm}$ and $P_{425\ nm}$, respectively. The amplitudes of the hematite ($I_{535\ nm}$) and goethite ($I_{425\ nm}$) were used for the relative concentrations of hematite and goethite, respectively (Scheinost, 1998). The concentration ratio of Hm/Gt is obtained by: $Hm/Gt = I_{535\ nm}/I_{425\ nm}$.

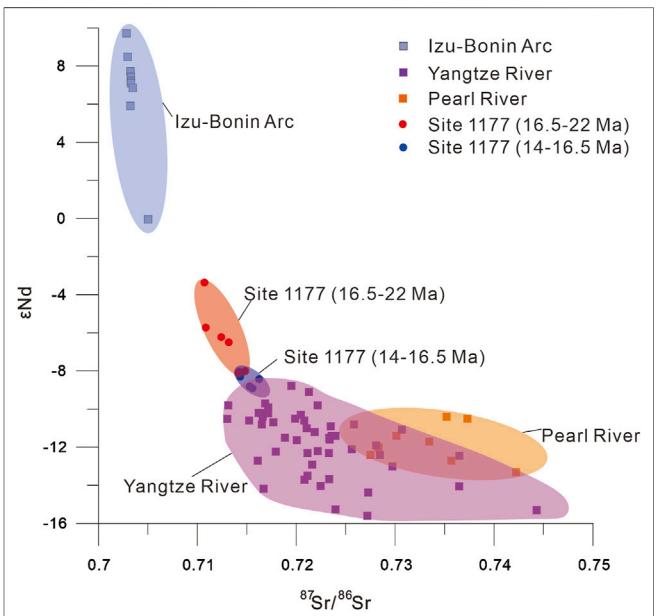

FIGURE 4 | The plot of $^{87}Sr/^{86}Sr$ and εNd for sediments from ODP Site 1177. Data for sediments from the Pearl River (Liu Z. et al., 2007), the Yangtze River (Yang et al., 2007; Meng et al., 2008), and the IBA (Tollstrup et al., 2010) are also shown for comparison.

RESULTS

The isotope, rock-magnetic parameter, and DRS results are shown in **Figures 3**, **4**. The εNd values range from −8.9 to −3.4 (**Figure 3A**). Before ~16.5 Ma, the εNd values are changeable and more positive, with an average εNd value of −6.3. After ~16.5 Ma, the εNd values are more stable and negative, with an average εNd value of −8.5. The plot of $^{87}Sr/^{86}Sr$ and εNd is shown in **Figure 4**. The data distribution can be divided into two clusters. The pre-16.5 Ma data are located in the middle part of the plot, while the post-16.5 Ma data are clustered in a region that near the Yangtze River (**Figure 4**).

In terms of the rock-magnetic parameters and DRS results, the *L*-ratio (**Figure 3B**) and $P_{425\ nm}$ (**Figure 3C**) could be divided into two parts. The *L*-ratios were overall greater than 0.13 before ~16.5 Ma and lesser than 0.13 since ~16.5 Ma, which indicates that the coercivity distribution of magnetic minerals changed at ~16.5 Ma. $P_{425\ nm}$ and $P_{535\ nm}$ are the characteristic band position of Gt and Hm, respectively. Variations in $P_{425\ nm}$ ($P_{535\ nm}$) values can be caused by different degrees of Al substitution (Hu et al., 2016). $P_{425\ nm}$ was relatively stable and was approximately 413 nm before ~16.5 Ma, and $P_{425\ nm}$ was variable and was larger than 413 nm after ~16.5 Ma. The temporal variations of $P_{425\ nm}$ indicate the different properties of Gt around ~16.5 Ma. The $P_{535\ nm}$ values were generally centered at 545 nm, except for a few points, and did not show an obvious first order shift trend before and after ~16.5 Ma (**Figure 3D**). The Hm/Gt ratios varied between 0 and 0.5 (**Figure 3E**). To compare with Site 1177, the trend of Hm/Gt ratios on Site 1148 (Clift et al., 2014) was shown (**Figure 3F**). Obviously, Sites 1148 and 1177 have different trends in Hm/Gt ratios.

The χ_{lf}, χ_{hf}, χ_{fd}, χ_{ARM}, SIRM, and χ_{ARM}/SIRM variations are shown in **Figures 3G–3L**. Although these rock-magnetic parameters are somewhat scattered, and could not be divided into two parts as clearly as *L*-ratio and $P_{425\ nm}$, there is still a rough transition point at ~16.5 Ma. The mean values of these magnetic parameters are also different before and after ~16.5 Ma. For example, before ~16.5 Ma, the mean values for χ_{lf}, χ_{hf}, χ_{fd}, χ_{ARM}, SIRM, and χ_{ARM}/SIRM are 9.02×10^{-8} m^3/kg, 8.96×10^{-8} m^3/kg, 6.90×10^{-10} m^3/kg, 2.81×10^{-8} m^3/kg, 1.74×10^{-4} Am^2/kg, and 2.56×10^{-4} A/m, respectively. After ~16.5 Ma, the mean values become χ_{lf} (1.05×10^{-7} m^3/kg), χ_{hf} (1.03×10^{-7} m^3/kg), χ_{fd} (1.65×10^{-9} m^3/kg), χ_{ARM} (1.12×10^{-8} m^3/kg), SIRM (3.48×10^{-4} Am^2/kg), and χ_{ARM}/SIRM (4.91×10^{-5} A/m). These differences imply different properties of magnetic minerals around ~16.5 Ma.

DISCUSSIONS

Overall, rock-magnetic, spectral, and geochemical parameters for sediments from the Site 1177 all shift at ~16.5 Ma in different degrees (**Figure 3**). Although different methods have inherent complexities in interpreting the sediment provenances, the combined method is the best approach to mutually attest to the potential changes in provenances.

First, the mineralogy, concentration, and grain size of magnetic minerals are tightly related to primary tectonic and/or environmental evolution (Liu et al., 2012). Variations in the magnetic parameters of sediments from Site 1177 indicate that the overall concentration of magnetic particles is larger (**Figures 3G–I**) and low-coercivity magnetic particles are coarser since ~16.5 Ma (**Figures 3B,**L), which suggests that there should be a crucial geological and/or environmental change at ~16.5 Ma.

The Philippine Sea is dominated by the sub-tropical East Asian monsoonal climate (Xu et al., 2012). Annual precipitation mostly occurs during the summer monsoon season (May–October) while dry winds prevail during the winter monsoon season (November–April) (Liu et al., 2009). Hm/Gt has been successfully employed as an indicator of subtropical East Asian monsoonal precipitation, the higher Hm/Gt, the less precipitation and weaker summer monsoon (e.g., Zhang et al., 2007; Gai et al., 2020). However, variations in the Hm/Gt record from Site 1177 share little similarity with that from the South China Sea Site 1148 (**Figures 3E,F**), which also locates in the subtropical East Asian monsoonal region (Clift et al., 2014). Differences between these two sites suggest that paleoclimate evolution cannot be used solely to explain the Hm/Gt record at Site 1177. Alternatively, geological processes such as sediment provenance and transportation changes should be taken into consideration. The mean *L*-ratio value is lower for sediment from the Site 1177 since ~16.5 Ma (**Figure 3B**), which indicates that coercivity of hard magnetic minerals (i.e., hematite and goethite) are changed systematically. Meanwhile, the characteristic DRS band position of goethite changed from approximately 413 nm to larger and variable wavelengths (**Figure 3C**), which indicates that the degree of Al substitution in goethite is increased and further explains the *L*-ratio value changes at ~16.5 Ma. That is, different degrees of Al substitution in goethite leads to changes in coercivity and affect the *L*-ratio values. Considering that the degree of Al substitution in antiferromagnetic minerals is correlated with the weathering condition in the material provenance (Hu et al., 2016), and the overall weathering condition is relatively stable (Clift et al., 2014), it is suggested that the shift of magnetic properties of sediments from the Site 1177 can be attributed to a provenance change.

Second, Sr and Nd isotopes are useful in tracing source changes (Wei et al., 2012; Clift et al., 2014). Clay mineral analyses suggested that the Izu-Bonin Arc was an important source for Site 1177 (Underwood and Fergusson, 2005). However, features of Sr-Nd isotopes from Site 1177 differ from that in the Izu-Bonin Arc, which indicates that the Izu-Bonin Arc cannot be the only provenance that feeds the Philippine Sea Plate and materials from other regions are needed to produce the Sr-Nd isotopic pattern in Site 1177. Liu et al. (2021) and Clift et al. (2013) suggested that the Pearl River and Yangtze River could provide materials to Site 1177. Therefore, we suggested that the early to middle Miocene provenances of Site 1177 were a mixture of the Izu-Bonin Arc, Pearl River, and Yangtze River. The pre-16.5 Ma and post-16.5 Ma Sr-Nd isotopes exhibit different patterns (**Figure 4**), which is consistent with variations in magnetic proxies at ~ 16.5 Ma (**Figures 3B–L**). The clay

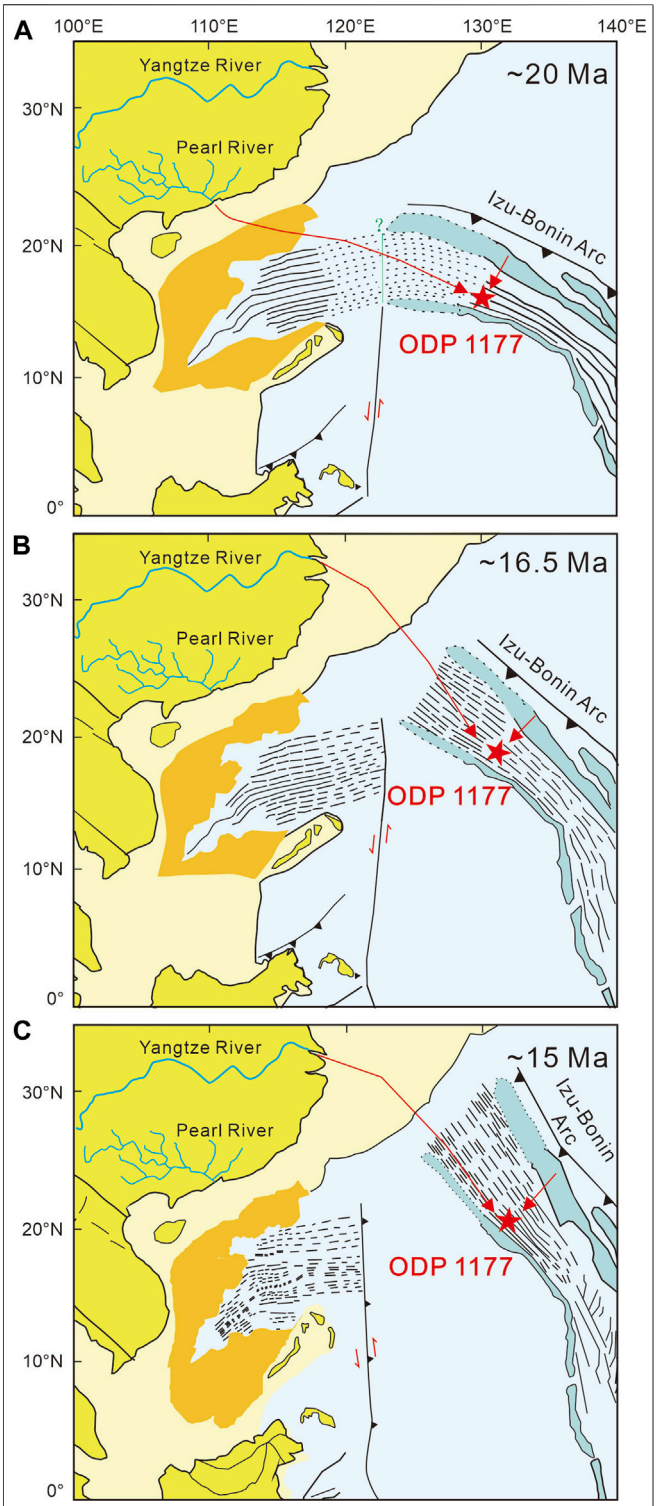

FIGURE 5 | The tectonic and provenance evolution of the Shikoku Basin at ~20 Ma (Liu et al., 2021), ~16.5 Ma (this study), and ~15 Ma (Liu et al., 2021). **(A)** The Shikoku Basin connected with the South China Sea, and Site 1177 received materials from the Pearl River and Izu-Bonin Arc at ~20 Ma. **(B)** The initial complete separation between the Shikoku Basin and the South China Sea was at ~16.5 Ma, and Site 1177 began to receive materials from the Yangtze River and Izu-Bonin Arc. **(C)** The Shikoku Basin moved further northward at ~15 Ma, and the provenance of Site 1177 was the same with that at ~ 16.5 Ma. The red arrows indicate the provenance directions. The dashed lines in **(A)** denote the recovered subducted slabs of the South China Sea (Zhao et al., 2019) and Shikoku Basin (Wu et al., 2016). To emphasize the relationships between the South China Sea and the Shikoku Basin, some ridges in the West Philippine Basin were not shown.

mineralogical data (**Figures 3M,N**) from Underwood and Fergusson (2005) also show detectable changes at ~16.5 Ma.

Third, zircons from the Pearl River and the Yangtze River were detected in Site 1177 turbidites deposited at ~18.6 Ma and ~15.4 Ma, respectively (Clift et al., 2013; Liu et al., 2021). The turbidites at ~18.6 Ma and ~15.4 Ma not only have different zircon age spectra, but they also have different lithologies, thicknesses of strata, stratigraphic units, and paleolatitudes. This implies that there was a provenance shift between ~18.6 Ma and ~15.4 Ma.

Given that the Izu-Bonin Arc has always been providing materials in the Miocene (Underwood and Fergusson, 2005), the shift of provenance could be attributed to the change of sources from Pearl River to Yangtze River. In fact, the Izu-Bonin Arc was oriented northwest and was at a relatively low latitude at ~20 Ma (Liu et al., 2021), which would prevent the transport of materials from the Yangtze River. Therefore, we suggest that mudstone materials in Site 1177 are sourced more from the Izu-Bonin Arc and the Pearl River before ~16.5 Ma, and from the Izu-Bonin Arc and the Yantze River after that.

The provenance evolutionary results are consistent with the paleomagnetic tectonic model that the Philippine Sea Plate experienced northward movement and clockwise rotation since the Eocene (Hall, 2002; Queano et al., 2007; Liu et al., 2021). It is obvious that the acceleration of the northward movement and clockwise rotation of the Philippine Sea Plate also occurred at approximately ~16.5 Ma (**Figures 3O–R**). Therefore, we suggest that the tectonic evolution plays a key role in the source shift at ~16.5 Ma for the studied site. Liu et al. (2021) proposed a model that the South China Sea was geographically connected to the Shikoku Basin at ~20 Ma (**Figure 5A**). Because of the collision between the Australian Plate and the Southeast Asia at ~20 Ma (Sdrolias et al., 2004) or ~23 Ma (Hall, 2011), the Shikoku Basin began to separate from the South China Sea. At ~15 Ma, the Shikoku Basin had completely separated from the South China Sea (**Figure 5C**). However, the initial time when the Shikoku Basin had completely separated from the South China Sea is unknown. Our new rock-magnetic, spectral, and geochemical analyses suggest that the provenance shift occurred significantly at ~ 16.5 Ma, which implies that the Shikoku Basin had thoroughly separated from the South China Sea at ~16.5 Ma (**Figure 5B**). Considering that the spreading of the South China Sea ceased at 16–15 Ma (Li et al., 2014), which is close to the full-separation time between the South China Sea and the Shikoku Basin at ~16.5 Ma, it is possible that these two tectonic events are attributed to an identical dynamic mechanism. The paleolatitude of the South China Block was relatively stable during the opening of the South China Sea (Huang et al., 2008), the stop spreading of the South China Sea should be related to the plate located south of the South China Sea.

The Australia plate, located to the south of the South China Sea and the Philippine Sea Plate, has been moving northward since the Cenozoic (Hall, 2002; Seton et al., 2012), which can not only explain the separation between the Shikoku Basin and the South China Sea but also account for the stop spreading of the South China Sea. With the Australian Plate moving northward, there is no room for the South China Sea to spread at 16–15 Ma, whereas the Shikoku Basin, with its subduction zone to the north, could move northward and clockwise rotate to sperate from the South China Sea. Underwood and Fergusson (2005), and Underwood and Pickering (2018) proposed that the Shikoku Basin was close to Japan and received sediments from Japan, the East China Sea, and the Izu-Bonin Arc since the middle Miocene. By combining our new results, we further suggest that the Shikoku Basin could have experienced considerable northward motion and clockwise rotation between the early Miocene and middle Miocene.

CONCLUSION

The provenances of sedimentary rocks from Site 1177 were comprehensively studied based on the temporal variations of geochemical, rock-magnetic, and spectral parameters from ~22 Ma to ~14 Ma. The results show that the provenance shifted at ~16.5 Ma. Before 16.5 Ma, mudstone materials mainly came from the Pearl River and Izu-Bonin Arc. After ~16.5 Ma, the materials originated from the Yangtze River and Izu-Bonin Arc. The provenance evolution is consistent with the Philippine Sea Plate tectonic model that the Shikoku Basin experienced northward motion and clockwise rotation in the Miocene, and the provenance shift constrains the time when the Shikoku Basin has been completely separated from the South China Sea at ~16.5 Ma.

DATA AVAILABILITY STATEMENT

The original contributions presented in the study are included in the article/Supplementary Material, further inquiries can be directed to the corresponding author.

AUTHOR CONTRIBUTIONS

QL designed the study and revised the manuscript. WL conducted the experiments, analyzed the data, and wrote the initial manuscript. CG helped to analyze the data and revised the manuscript. WF, YAZ, YIZ, WC, and YL helped to analyze the data. XZ revised the manuscript.

FUNDING

This study was supported by the National Natural Science Foundation of China (92158208, 41874076, 41874078, 42002052, 41704068), the China Postdoctoral Science Foundation (2021M701557), the opening foundation (SSKP202101) of the Shanghai Sheshan National Geophysical Observatory, Shanghai, China, and the Shenzhen Science and Technology Program (KQTD20170810111725321).

ACKNOWLEDGMENTS

Samples in this research were provided by the Ocean Drilling Program (ODP). We thank Prof. Minghui Zhao and Prof. Jian Lin provided good suggestions.

REFERENCES

Arculus, R. J., Ishizuka, O., Bogus, K. A., Gurnis, M., Hickey-Vargas, R., Aljahdali, M. H., et al. (2015). A Record of Spontaneous Subduction Initiation in the Izu-Bonin-Mariana Arc. *Nat. Geosci.* 8, 728–733. doi:10.1038/NGEO2515

Bleil, U. (1982). Paleomagnetism of Deep Sea Drilling Project Leg 60 Sediments and Igneous Rocks from the Mariana Region. *Initial Rep. Deep Sea Drill. Proj.* 60, 1982. doi:10.2973/DSDP.PROC.60.152.1982

Chen, Y., Niu, Y., Xue, Q., Gao, Y., and Castillo, P. (2021). An Iron Isotope Perspective on Back-Arc Basin Development: Messages from Mariana Trough Basalts. *Earth Planet. Sci. Lett.* 572, 117133. doi:10.1016/J.EPSL.2021.117133

Clift, P. D., Carter, A., Nicholson, U., and Masago, H. (2013). Zircon and Apatite Thermochronology of the Nankai Trough Accretionary Prism and Trench, Japan: Sediment Transport in an Active and Collisional Margin Setting. *Tectonics* 32, 377–395. doi:10.1002/tect.20033

Clift, P. D., Wan, S., and Blusztajn, J. (2014). Reconstructing Chemical Weathering, Physical Erosion and Monsoon Intensity since 25Ma in the Northern South China Sea: A Review of Competing Proxies. *Earth-Science Rev.* 130, 86–102. doi:10.1016/j.earscirev.2014.01.002

Deschamps, A., and Lallemand, S. (2002). The West Philippine Basin: An Eocene to Early Oligocene Back Arc Basin Opened between Two Opposed Subduction Zones. *J. Geophys. Res.* 107, 1. doi:10.1029/2001jb001706

Fagel, N., Robert, C., Preda, M., and Thorez, J. (2001). Smectite Composition as a Tracer of Deep Circulation: the Case of the Northern North Atlantic. *Mar. Geol.* 172, 309–330. doi:10.1016/S0025-3227(00)00123-7

Gai, C., Liu, Q., Roberts, A. P., Chou, Y., Zhao, X., Jiang, Z., et al. (2020). East Asian Monsoon Evolution since the Late Miocene from the South China Sea. *Earth Planet. Sci. Lett.* 530, 115960. doi:10.1016/J.EPSL.2019.115960

Goldstein, S. J., and Jacobsen, S. B. (1988). Nd and Sr Isotopic Systematics of River Water Suspended Material: Implications for Crustal Evolution. *Earth Planet. Sci. Lett.* 87, 249–265. doi:10.1016/0012-821X(88)90013-1

Hall, R., Ali, J. R., Anderson, C. D., and Baker, S. J. (1995). Origin and Motion History of the Philippine Sea Plate. *Tectonophysics* 251, 229–250. doi:10.1016/0040-1951(95)00038-0

Hall, R. (2011). Australia-SE Asia Collision: Plate Tectonics and Crustal Flow. *Geol. Soc. Lond. Spec. Publ.* 355, 75–109. doi:10.1144/SP355.5

Hall, R. (2002). Cenozoic Geological and Plate Tectonic Evolution of SE Asia and the SW Pacific: Computer-Based Reconstructions, Model and Animations. *J. Asian Earth Sci.* 20, 353–431. doi:10.1016/S1367-9120(01)00069-4

Haston, R. B., and Fuller, M. (1991). Paleomagnetic Data from the Philippine Sea Plate and Their Tectonic Significance. *J. Geophys. Res.* 96, 6073–6098. doi:10.1029/90JB02700

Haston, R. B., Stokking, L. B., and Ali, J. (1992). Paleomagnetic Data from Holes 782A, 784A, and 786A, Leg 125. *Proc. Ocean Drill. ProgramScientific Results* 125, 535–545. doi:10.2973/odp.proc.sr.125.156.1992

Hilde, T. W. C., and Chao-Shing, L. (1984). Origin and Evolution of the West Philippine Basin: A New Interpretation. *Tectonophysics* 102, 85–104. doi:10.1016/0040-1951(84)90009-X

Hu, P., Jiang, Z., Liu, Q., Heslop, D., Roberts, A. P., Torrent, J., et al. (2016). Estimating the Concentration of Aluminum-substituted Hematite and Goethite Using Diffuse Reflectance Spectrometry and Rock Magnetism: Feasibility and Limitations. *J. Geophys. Res. Solid Earth* 121, 4180–4194. doi:10.1002/2015JB012635

Huang, B. C., Zhou, Y. X., and Zhu, R. X. (2008). Discussions on Phanerozoic Evolution and Formation of Continental China, Based on Paleomagnetic Studies (In Chinese with English Abstract). *Earth Sci. Front.* 15, 348–359. doi:10.3321/j.issn:1005-2321.2008.03.031

Hussong, D. M., and Uyeda, S. (1982). Tectonic Processes and the History of the Mariana Arc: A Synthesis of the Results of Deep Sea Drilling Project Leg 60. *Initial Rep. Deep Sea Drill. Proj.* 60, 1982. doi:10.2973/DSDP.PROC.60.154.1982

Ishizuka, O., Taylor, R. N., Ohara, Y., and Yuasa, M. (2013). Upwelling, Rifting, and Age-Progressive Magmatism from the Oki-Daito Mantle Plume. *Geology* 41, 1011–1014. doi:10.1130/G34525.1

Keating, B., and Herrero, E. (1981). Paleomagnetic Studies of Basalts and Andesites from Deep Sea Drilling Project Leg 59. *Initial Rep. Deep Sea Drill. Proj.* 59, 1981. doi:10.2973/DSDP.PROC.59.113.1981

Keating, B. (1981). Paleomagnetic Study of Sediments from Deep Sea Drilling Project Leg 59. *Initial Rep. Deep Sea Drill. Proj.* 59, 1981. doi:10.2973/DSDP.PROC.59.112.1981

Kinoshita, H. (1980). Paleomagnetism of Sediment Cores from Deep Sea Drilling Project Leg 58, Philippine Sea. *Initial. Rep. Deep Sea Drill. Proj.* 58, 765–768. doi:10.2973/dsdp.proc.58.128.1980

Koyama, M., Cisowski, S. M., and Pezard, P. (1992). Paleomagnetic Evidence for Northward Drift and Clockwise Rotation of the Izu-Bonin Forearc since the Early Oligocene. *Sci. Results* 126, 353–370. doi:10.2973/odp.proc.sr.126.143.1992

Lallemand, S. (2016). Philippine Sea Plate Inception, Evolution, and Consumption with Special Emphasis on the Early Stages of Izu-Bonin-Mariana Subduction. *Prog. Earth Planet. Sci.* 3, 15. doi:10.1186/s40645-016-0085-6

Li, C.-F., Xu, X., Lin, J., Sun, Z., Zhu, J., Yao, Y., et al. (2014). Ages and Magnetic Structures of the South China Sea Constrained by Deep Tow Magnetic Surveys and IODP Expedition 349. *Geochem. Geophys. Geosyst.* 15, 4958–4983. doi:10.1002/2014GC005567

Li, H., Arculus, R. J., Ishizuka, O., Hickey-Vargas, R., Yogodzinski, G. M., McCarthy, A., et al. (2021). Basalt Derived from Highly Refractory Mantle Sources during Early Izu-Bonin-Mariana Arc Development. *Nat. Commun.* 12, 1723. doi:10.1038/S41467-021-21980-0

Liu, Q., Roberts, A. P., Larrasoaña, J. C., Banerjee, S. K., Guyodo, Y., Tauxe, L., et al. (2012). Environmental Magnetism: Principles and Applications. *Rev. Geophys.* 50, 393. doi:10.1029/2012RG000393

Liu, Q., Roberts, A. P., Torrent, J., Horng, C.-S., and Larrasoaña, J. C. (2007a). What Do the HIRM andS-Ratio Really Measure in Environmental Magnetism? *Geochem. Geophys. Geosyst.* 8, a–n. doi:10.1029/2007GC001717

Liu, W., Gai, C., Feng, W., Cao, W., Guo, L., Zhong, Y., et al. (2021). Coeval Evolution of the Eastern Philippine Sea Plate and the South China Sea in the Early Miocene: Paleomagnetic and Provenance Constraints from ODP Site 1177. *Geophys. Res. Lett.* 48, e2021GL093916. doi:10.1029/2021GL093916

Liu, Z., Colin, C., Huang, W., Le, K. P., Tong, S., Chen, Z., et al. (2007b). Climatic and Tectonic Controls on Weathering in South China and Indochina Peninsula: Clay Mineralogical and Geochemical Investigations from the Pearl, Red, and Mekong Drainage Basins. *Geochem. Geophys. Geosyst.* 8, a–n. doi:10.1029/2006GC001490

Liu, Z., Zhao, Y., Colin, C., Siringan, F. P., and Wu, Q. (2009). Chemical Weathering in Luzon, Philippines from Clay Mineralogy and Major-Element Geochemistry of River Sediments. *Appl. Geochem.* 24, 2195–2205. doi:10.1016/j.apgeochem.2009.09.025

Louden, K. E. (1977). Paleomagnetism of DSDP Sediments, Phase Shifting of Magnetic Anomalies, and Rotations of the West Philippine Basin. *J. Geophys. Res.* 82, 2989–3002. doi:10.1029/JB082I020P02989

Ma, P., Liu, S., Gurnis, M., and Zhang, B. (2019). Slab Horizontal Subduction and Slab Tearing beneath East Asia. *Geophys. Res. Lett.* 46, 5161–5169. doi:10.1029/2018GL081703

Maunder, B., Prytulak, J., Goes, S., and Reagan, M. (2020). Rapid Subduction Initiation and Magmatism in the Western Pacific Driven by Internal Vertical Forces. *Nat. Commun.* 11, 1874. doi:10.1038/S41467-020-15737-4

Meng, X., Liu, Y., Shi, X., and Du, D. (2008). Nd and Sr Isotopic Compositions of Sediments from the Yellow and Yangtze Rivers: Implications for Partitioning Tectonic Terranes and Crust Weathering of the Central and Southeast China. *Front. Earth Sci. China* 2, 418–426. doi:10.1007/s11707-008-0054-5

Okino, K., Ohara, Y., Kasuga, S., and Kato, Y. (1999). The Philippine Sea: New Survey Results Reveal the Structure and the History of the Marginal Basins. *Geophys. Res. Lett.* 26, 2287–2290. doi:10.1029/1999GL900537

Queano, K. L., Ali, J. R., Milsom, J., Aitchison, J. C., and Pubellier, M. (2007). North Luzon and the Philippine Sea Plate Motion Model: Insights Following Paleomagnetic, Structural, and Age-Dating Investigations. *J. Geophys. Res.* 112, 4506. doi:10.1029/2006JB004506

Queaño, K. L., Yumul Jr., G. P., Marquez, E. J., Gabo-Ratio, J. A., Payot, B. D., and Dimalanta, C. B. (2020). Consumed Tectonic Plates in Southeast Asia: Markers from the Mesozoic to Early Cenozoic Stratigraphic Units in the Northern and Central Philippines. *J. Asian Earth Sci. X* 4, 100033. doi:10.1016/j.jaesx.2020.100033

Reagan, M. K., Ishizuka, O., Stern, R. J., Kelley, K. A., Ohara, Y., Blichert-Toft, J., et al. (2010). Fore-arc Basalts and Subduction Initiation in the Izu-Bonin-Mariana System. *Geochem. Geophys. Geosyst.* 11, a–n. doi:10.1029/2009GC002871

Richter, C., and Ali, J. R. (2015). Philippine Sea Plate Motion History: Eocene-Recent Record from ODP Site 1201, Central West Philippine Basin. *Earth Planet. Sci. Lett.* 410, 165–173. doi:10.1016/j.epsl.2014.11.032

Saitoh, Y., Ishikawa, T., Tanimizu, M., Murayama, M., Ujiie, Y., Yamamoto, Y., et al. (2015). Sr, Nd, and Pb Isotope Compositions of Hemipelagic Sediment in the Shikoku Basin: Implications for Sediment Transport by the Kuroshio and Philippine Sea Plate Motion in the Late Cenozoic. *Earth Planet. Sci. Lett.* 421, 47–57. doi:10.1016/j.epsl.2015.04.001

Sasaki, T., Yamazaki, T., and Ishizuka, O. (2014). A Revised Spreading Model of the West Philippine Basin. *Earth Planet Sp.* 66, 83. doi:10.1186/1880-5981-66-83

Scheinost, A. C. (1998). Use and Limitations of Second-Derivative Diffuse Reflectance Spectroscopy in the Visible to Near-Infrared Range to Identify and Quantify Fe Oxide Minerals in Soils. *Clays Clay Minerals* 46, 528–536. doi:10.1346/CCMN.1998.0460506

Sdrolias, M., Roest, W. R., and Müller, R. D. (2004). An Expression of Philippine Sea Plate Rotation: The Parece Vela and Shikoku Basins. *Tectonophysics* 394, 69–86. doi:10.1016/j.tecto.2004.07.061

Seton, M., Müller, R. D., Zahirovic, S., Gaina, C., Torsvik, T., Shephard, G., et al. (2012). Global Continental and Ocean Basin Reconstructions since 200Ma. *Earth-Science Rev.* 113, 212–270. doi:10.1016/j.earscirev.2012.03.002

Shipboard Scientific Party (2001). Site 1177. *Proc. Ocean Drill. Program* 190, 1–91. doi:10.2973/odp.proc.ir.190.108.2001

Sibuet, J.-C., Zhao, M., Wu, J., and Lee, C.-S. (2021). Geodynamic and Plate Kinematic Context of South China Sea Subduction during Okinawa Trough Opening and Taiwan Orogeny. *Tectonophysics* 817, 229050. doi:10.1016/J.TECTO.2021.229050

Steurer, J. F., and Underwood, M. B. (2003). Clay Mineralogy of Mudstones from the Nankai Trough Reference Sites 1173 and 1177 and Frontal Accretionary Prism Site 1174. *Sci. Results* 190/196, 1–37. doi:10.2973/odp.proc.sr.190196.211.2003

Tollstrup, D., Gill, J., Kent, A., Prinkey, D., Williams, R., Tamura, Y., et al. (2010). Across-arc Geochemical Trends in the Izu-Bonin Arc: Contributions from the Subducting Slab, Revisited. *Geochem. Geophys. Geosyst.* 11, a–n. doi:10.1029/2009GC002847

Underwood, M. B., and Fergusson, C. L. (2005). Late Cenozoic Evolution of the Nankai Trench-Slope System: Evidence from Sand Petrography and Clay Mineralogy. *Geol. Soc. Lond. Spec. Publ.* 244, 113–129. doi:10.1144/GSL.SP.2005.244.01.07

Underwood, M. B., and Pickering, K. T. (2018). Facies Architecture, Detrital Provenance, and Tectonic Modulation of Sedimentation in the Shikoku Basin: Inputs to the Nankai Trough Subduction Zone. *Spec. Pap. Geol. Soc. Am.* 534, 1–34. doi:10.1130/2018.2534(01

Wei, G., Liu, Y., Ma, J., Xie, L., Chen, J., Deng, W., et al. (2012). Nd, Sr Isotopes and Elemental Geochemistry of Surface Sediments from the South China Sea: Implications for Provenance Tracing. *Mar. Geol.* 319-322, 21–34. doi:10.1016/j.margeo.2012.05.007

Wu, J., Suppe, J., Lu, R., and Kanda, R. (2016). Philippine Sea and East Asian Plate Tectonics since 52 Ma Constrained by New Subducted Slab Reconstruction Methods. *J. Geophys. Res. Solid Earth* 121, 4670–4741. doi:10.1002/2016JB012923

Xu, Z., Li, T., Wan, S., Nan, Q., Li, A., Chang, F., et al. (2012). Evolution of East Asian Monsoon: Clay Mineral Evidence in the Western Philippine Sea over the Past 700kyr. *J. Asian Earth Sci.* 60, 188–196. doi:10.1016/j.jseaes.2012.08.018

Yamazaki, T., Chiyonobu, S., Ishizuka, O., Tajima, F., Uto, N., and Takagawa, S. (2021). Rotation of the Philippine Sea Plate Inferred from Paleomagnetism of Oriented Cores Taken with an ROV-Based Coring Apparatus. *Earth Planets Space* 73, 1–10. doi:10.1186/S40623-021-01490-5

Yamazaki, T., Seama, N., Okino, K., Kitada, K., Joshima, M., Oda, H., et al. (2003). Spreading Process of the Northern Mariana Trough: Rifting-Spreading Transition at 22°N. *Geochem. Geophys. Geosyst.* 4, a–n. doi:10.1029/2002GC000492

Yamazaki, T., Takahashi, M., Iryu, Y., Sato, T., Oda, M., Takayanagi, H., et al. (2010). Philippine Sea Plate Motion since the Eocene Estimated from Paleomagnetism of Seafloor Drill Cores and Gravity Cores. *Earth Planet Sp.* 62, 495–502. doi:10.5047/eps.2010.04.001

Yang, S., Jiang, S., Ling, H., Xia, X., Sun, M., and Wang, D. (2007). Sr-Nd Isotopic Compositions of the Changjiang Sediments: Implications for Tracing Sediment Sources. *Sci. China Ser. D.* 50, 1556–1565. doi:10.1007/s11430-007-0052-6

Zahirovic, S., Seton, M., and Müller, R. D. (2014). The Cretaceous and Cenozoic Tectonic Evolution of Southeast Asia. *Solid earth.* 5, 227–273. doi:10.5194/se-5-227-2014

Zhang, Y. G., Ji, J., Balsam, W. L., Liu, L., and Chen, J. (2007). High Resolution Hematite and Goethite Records from ODP 1143, South China Sea: Co-evolution of Monsoonal Precipitation and El Niño over the Past 600,000 Years. *Earth Planet. Sci. Lett.* 264, 136–150. doi:10.1016/J.EPSL.2007.09.022

Zhao, M., Sibuet, J.-C., and Wu, J. (2019). Intermingled Fates of the South China Sea and Philippine Sea Plate. *Natl. Sci. Rev.* 6, 886–890. doi:10.1093/nsr/nwz107

Conflict of Interest: The authors declare that the research was conducted in the absence of any commercial or financial relationships that could be construed as a potential conflict of interest.

Publisher's Note: All claims expressed in this article are solely those of the authors and do not necessarily represent those of their affiliated organizations, or those of the publisher, the editors and the reviewers. Any product that may be evaluated in this article, or claim that may be made by its manufacturer, is not guaranteed or endorsed by the publisher.